

Modification of nonequilibrium fluctuations by interaction with surfaces

Glen Satten and David Ronis

Department of Chemistry, Harvard University, 12 Oxford Street, Cambridge, Massachusetts 02138

(Received 16 October 1981)

Fluctuating hydrodynamics is used to calculate the density correlation function and light-scattering spectrum for a fluid in a stationary temperature gradient. The non-plane-wave nature of the light source in the direction of the temperature gradient is considered explicitly. Finite-size effects are shown to be important when the ratio of system size to dynamic correlation length is smaller than or equal to $O(1)$. The magnitude and size of the asymmetry of the Brillouin peaks, as well as the line shapes, are found to depend strongly on the scattering wave vector, beam width, and system size, while the dependence on the surface reflection coefficient is much weaker than expected. The importance of including surface fluctuations when absorbing walls are used is discussed.

I. INTRODUCTION

Recently, several papers have discussed the light-scattering spectrum of a fluid in a stationary temperature gradient using the fluctuating hydrodynamics method.¹⁻⁵ In all cases, the effect of the boundary of the fluid has been ignored by assuming that the size of the fluid in the direction of the temperature gradient (denoted by L) is much larger than any other characteristic length scale in the problem. In this limit, an asymmetry in the integrated intensities of the Brillouin peaks ($I_{>,<}$) is predicted; in addition, all linear theories agree that the quantitative measure of the asymmetry ϵ is given by¹⁻⁸

$$\epsilon = \frac{I_{>} - I_{<}}{I_{>} + I_{<}} = \frac{|\vec{\nabla}T| c_0 q}{\alpha T_0 k^3}, \quad (1)$$

where c_0 is the speed of sound in the fluid, α is the kinematic sound attenuation coefficient, and q is the component of the wave vector \vec{k} in the direction of the temperature gradient $\vec{\nabla}T$. This result is in agreement with calculations using nonlinear-response theory^{6,7} and kinetic theory.^{8,9} Qualitatively, this effect arises because there is a net flux of phonons traveling from the hot to the cold wall.

Unfortunately, the only experiments¹⁰ to test this prediction were carried out under conditions for which L was not the largest length scale (in particular, the mean-free path of the phonons l was larger). The consequent disagreement between the observed and predicted asymmetry was attributed to mode-coupling effects. In this paper we will show that

the inclusion of the finite size of the fluid in the direction of the temperature gradient has a large effect on the magnitude of ϵ which can reconcile the experimental results with linear theory. Qualitatively, we expect a decrease in ϵ due to boundary effects, as reflection of phonons will tend to cancel the net flux of phonons traveling away from the hot boundary. In addition, because the system is finite, fewer phonons will be collected from very hot ($x > L/2$) or very cold ($x < -L/2$) regions, further reducing the asymmetry.

In addition, most theories to date neglect the non-plane-wave character of a real light source when calculating the light-scattering spectrum. A notable exception is the work of Tremblay *et al.*,^{2(b)} in which the effect of a Gaussian light source is considered. The light source may only be treated as a plane wave if both the wavelength and the mean-free path of the scattering phonons are much smaller than the beamwidth. With the above exception, all previous work has only included the possibility of incorporating a finite beam at the formal level, the actual spectra being computed as if the beam were much wider than the dynamic correlation length l . This results in line shapes which are Lorentzian or the square of Lorentzian. For the systems used by Beysens *et al.* the mean-free path of the phonons is approximately 2 cm. Thus, for the plane-wave approximation to be valid, a beam of at least 5 cm width must be used. Rather than impose this restriction on the experiment, we have explicitly included the finite size of the beam by assuming that the light source has a Gaussian profile in the direction of the temperature gradient. The

only assumption on length scales is that the halfwidth of the light beam d be less than L . It will be seen that the line shape of the Brillouin peaks in regions of physical interest is determined primarily by the characteristics of the light source. This is in agreement with Ref. 2(b). (For further discussion of the nonobservability of natural line shapes, see Ref. 3.) In Sec. II we outline the general theory and calculate the density correlation function. In Sec. III we derive the light-scattering spectrum using the results of Sec. II. In Sec. IV we discuss the spectra generated by the results of Sec. III, and compare our results with the experimental results by Beysens *et al.* In Sec. V we present additional comments and concluding remarks.

II. GENERAL THEORY AND THE DENSITY CORRELATION FUNCTION

In fluctuating hydrodynamics,¹¹ fluctuations are assumed to evolve under the linearized Navier-Stokes equations with white-noise source terms. To simplify the equations of motion, we assume that the thermal expansion coefficient is zero. For an infinite fluid, this leads to the following equation for the density fluctuation:

$$\frac{\partial^2 \rho}{\partial t^2} - c_0^2 \nabla^2 \rho - \alpha \nabla^2 \frac{\partial \rho}{\partial t} = \nabla^2 \tau, \quad (2)$$

where c_0 and α (assumed constant) are as above, and τ is the longitudinal component of the fluctuating stress tensor (white-noise source), which can be shown to have the following nonequilibrium correlation function^{1,11}:

$$\begin{aligned} \langle \tau(\vec{r}, t) \tau(\vec{r}', t') \rangle_{\text{NE}} \\ = 2k_B \rho_0 \alpha T(\vec{r}) \delta(\vec{r} - \vec{r}') \delta(t - t'). \end{aligned} \quad (3)$$

Fourier transforming Eq. (2) in x , y , z , and t leads directly to the linear prediction for ϵ in the (infinite) fluid [Eq. (1)]. For this paper, however, we assume the fluid is infinite in the y and z direction only, which leads to Eq. (4):

$$\frac{\partial^2 \tilde{\rho}}{\partial x^2} + \kappa^2 \tilde{\rho} = -\frac{1}{c_\omega^2} \left[\frac{\partial^2 \tilde{\tau}}{\partial x^2} - k_{||}^2 \tilde{\tau} \right], \quad (4)$$

$$\tilde{\rho}(x, \vec{k}_{||}, \omega) = \int_{-\infty}^{\infty} \rho(\vec{r}, t) e^{i\omega t - i\vec{k}_{||} \cdot \vec{r}} d^2 r_{||} dt,$$

where $c_\omega^2 = c_0^2 - i\omega\alpha$ and $\kappa^2 = \omega^2/c_\omega^2 - \vec{k}_{||}^2$.

For a finite fluid, Eqs. (2)–(4) are incomplete at the fluctuating level if dissipation occurs at the boundaries (i.e., if the walls are not totally reflecting). Physically, this comes about because the walls absorb some of the fluctuations generated in the fluid but do not transmit to the fluid any fluctuations generated in the walls. As a result, the fluctuation-dissipation theorem is not obeyed, and in particular, time-reversal symmetry is violated in equilibrium. To compensate for this, we add fluctuating source terms, σ , localized at each boundary ($x = \pm L/2$). Since these terms model fluctuations originating above and below the fluid, they are assumed to be statistically independent of the fluctuating stress tensor in the bulk of the fluid, and of each other.¹² An equivalent approach would be to consider the fluctuating dynamics of the combined fluid-wall system. This approach has been used by van Vliet *et al.*¹³ in considering the noise spectrum in a thin film on a substrate. In practice, however, this method is limited to surfaces which are smooth with respect to all other length scales. To avoid this restriction, we will use surface source terms, and model the effect of the solid on the fluid through phenomenological boundary conditions. Thus, our equation for the density fluctuation in the fluid is

$$\begin{aligned} \frac{\partial^2 \tilde{\rho}}{\partial x^2} + \kappa^2 \tilde{\rho} \\ = \frac{-1}{c_\omega^2} \left[\frac{\partial^2 \tilde{\tau}}{\partial x^2} - k_{||}^2 \tilde{\tau} + \tilde{\sigma}(L/2) \delta(x - L/2) \right. \\ \left. + \tilde{\sigma}(-L/2) \delta(x + L/2) \right]. \end{aligned} \quad (5)$$

For the moment, we will postpone the discussion of the statistical properties of $\tilde{\sigma}$. As we shall show [cf. Eq. (14') below], only very limited information regarding the statistical behavior of the random noise fluctuations at the surfaces is needed to compute the density correlation function. The required information will be obtained by insisting that the equilibrium density correlation function must be even under time reversal, even in a finite system. The generalization to the nonequilibrium regime is then analogous to Eq. (3).

The solution to Eq. (5) for a fluid confined between boundaries at $x = \pm L/2$ can be expressed in terms of the Green's function

$$\tilde{\rho}(x, \vec{k}_{||}, \omega) = - \int_{-L/2}^{L/2} G(\vec{k}_{||}, x, x', \omega) \frac{1}{c_\omega^2} \left[\left[\frac{\partial^2 \tilde{\tau}}{\partial x'^2} \right] - k_{||}^2 \tilde{\tau} \right] dx' - \frac{G(x | L/2) \tilde{\sigma}(L/2) + G(x | -L/2) \tilde{\sigma}(-L/2)}{c_\omega^2} \quad (6)$$

$$G(\vec{k}_{||}, x, x', \omega) = \frac{\cos \kappa(x_> - L/2 + \phi) \cos \kappa(x_< + L/2 - \phi)}{\kappa \sin \kappa(L - 2\phi)} \quad (7)$$

where $x_> = \max(x, x')$, $x_< = \min(x, x')$. The phase ϕ is determined by the acoustic boundary condition

$$\frac{\partial \tilde{G}}{\partial x} = \pm \frac{i\omega\beta G}{c_0} \quad \text{for } x = \pm L/2 \quad (8)$$

where β is the (complex) specific acoustic admittance of the boundary.¹⁴ To simplify the calculation, we have assumed the acoustic admittance is independent of temperature.

Integrating Eq. (6) by parts, using Eq. (8) and the defining equation for \tilde{G} gives

$$\tilde{\rho}(x, \vec{k}_{||}, \omega) = - \sum_{\pm} \frac{G(x | \pm L/2)}{c_\omega^2} \left[\pm \frac{\partial \tilde{\tau}}{\partial x'} + \tilde{\sigma} - \frac{i\omega\beta}{c_0} \tilde{\tau} \right]_{x' = \pm L/2} - \frac{1}{c_\omega^2} \tilde{\tau}(x) + \frac{\omega^2}{c_\omega^4} \int_{-L/2}^{L/2} dx_1 G(x | x_1) \tilde{\tau}(x_1) \quad (9)$$

The specific acoustic admittance of a smooth planar solid-liquid boundary can be calculated theoretically if the solid is modeled as an elastic continuum. The total admittance is expressed as the sum of two terms, the first arising from the solid-liquid interface itself, and the second from coupling to the transverse velocity modes in a thin boundary layer at the surface. The interface admittance is given by¹⁴

$$\beta_I = \frac{\rho_0 c_0}{\rho_s c_l} \left\{ \frac{\left[1 - 2 \left[\frac{c_s \sin \theta}{c_0} \right]^2 \right]^2}{\left[1 - \left[\frac{c_l \sin \theta}{c_0} \right]^2 \right]^{1/2}} + 4 \frac{c_s}{c_l} \left[\frac{c_s \sin \theta}{c_0} \right]^2 \left[1 - \left[\frac{c_s \sin \theta}{c_0} \right]^2 \right]^{1/2} \right\}^{-1} \quad (10)$$

where ρ_0 is the density of fluid, ρ_s is the density of the solid, c_0 is the sound velocity in the fluid, c_l is the longitudinal-wave velocity in the solid, c_s is the shear-wave velocity in the solid, $\theta = \sin^{-1}(\omega \vec{k}_{||}/c_0) =$ angle of incidence. The boundary-layer admittance is given by¹²

$$\beta_{BL} = e^{-i\pi/4} \left[\frac{\omega \eta}{\rho_0 c_0^2} \right]^{1/2} \sin^2 \theta \quad (11)$$

where η is the fluid viscosity. Note that for normal incidence ($k_{||} = 0$), the acoustic admittance is given simply by

$$\beta_{tot} = \frac{\rho_0 c_0}{\rho_s c_l} \quad (12)$$

The acoustic admittance is related simply to the reflection coefficient R by

$$R = \frac{\cos \theta - \beta}{\cos \theta + \beta} \quad (13)$$

where θ is the angle of incidence of the scattering phonon. In this paper we will consider only the case $\theta = 0$, although the results of this paper hold for $\theta \neq 0$ as well. For the system studied experimentally, Eq. (12) predicts $\beta = 0.03$.

Strictly speaking, the acoustic impedance calculated by Eqs. (10)–(12) can only be applied when the surface is smooth on the scale of the phonon wavelength. For light scattering, this corresponds to the requirement that the surface roughness be less than $\sim 10 \mu\text{m}$. Unfortunately, the surface roughness in the only experiment to date is $\sim 100 \mu\text{m}$. Thus, β cannot be calculated by the simple elastic theory given above, but can be determined experimentally.¹⁴ In comparing with experimental results, we have presented a minimum and maximum ϵ (corresponding to $\beta = 0$, $R = 1$ and $\beta = 1$, $R = 0$, respectively) as well as a value corresponding to about 33% reflection ($\beta = 0.5$).

From Eqs. (3) and (9), we obtain the density correlation function

$$\begin{aligned} \frac{\langle \tilde{\rho}(x, \vec{k}_{||}, \omega) \tilde{\rho}^*(x', \vec{k}_{||}, \omega) \rangle_{\text{NE}}}{2k_B \rho_0 \alpha} &= \frac{1}{|c_\omega|^4} T(x) \delta(x-x') - \frac{\omega^2}{|c_\omega|^4} \left[\frac{G(x|x') T(x')}{c_\omega^2} + \frac{G^*(x'|x) T(x)}{(c_\omega^*)^2} \right] \\ &+ \frac{\omega^4}{|c_\omega|^8} \int_{-L/2}^{L/2} dx_1 G(x|x_1) T(x_1) G^*(x'|x_1) \\ &+ \sum_{\pm} \frac{\Sigma(\pm L/2) T(\pm L/2)}{|c_\omega|^4 \alpha} G(x|\pm L/2) G^*(x'|\pm L/2), \end{aligned} \quad (14)$$

where

$$\begin{aligned} 2k_B \Sigma(\pm L/2) T(\pm L/2) &\equiv \left\langle \left| \pm \frac{\partial \tilde{\tau}}{\partial x} + \tilde{\sigma} - \frac{i\omega\beta}{c_0} \tilde{\tau} \right|_{x=\pm L/2}^2 \right\rangle_{\text{NE}} \\ &- \omega^2 \int_{-L/2}^{L/2} dx \left[\frac{\langle \tilde{\tau}(x) \left[\pm \frac{\partial \tau}{\partial x_1} + \tilde{\sigma} - \frac{i\omega\beta}{c_0} \tilde{\tau} \right]_{x_1=\pm L/2} \rangle_{\text{NE}}}{c_\omega^2} + \text{cc} \right]. \end{aligned} \quad (14')$$

In obtaining Eq. (14), we have assumed that correlations between $\tau(x)$ and the surface random noise at $\pm(L/2)$ is localized to within a microscopic distance of the surface and vanishes in the bulk. This assumption is reasonable given that the random sources are supposed to represent microscopic scale fluctuations (i.e., in τ , etc.) and thus should correlate only over microscopic distances and times. This is also the rationale behind the δ function in Eq. (3).^{1,11} Finally, we have omitted two terms in Eq. (14) which are nonzero only if x or x' is on the surface.

From Eq. (14') we see (as mentioned above) that of the myriad of random surface source correlations which would, in general, need to be specified in order to completely solve the stochastic problem posed by Eq. (5), only a very specific combination of them is required for the density-density correlation function. If we had started by first phenomenologically specifying the surface correlations, we see that there are an infinite number of equivalent choices which would give the same value for Σ and hence same physical observable correlation function. This is no accident and arises partly due to the fact that the decomposition of the noise into surface δ -function source and random stress is somewhat *ad hoc*; the sum being the only relevant quantity [cf. Eq. (5)].

Finally, in the spirit of Eq. (3), we assume that Σ may be replaced by its equilibrium value. The fact that the system is out of equilibrium is reflected by the explicit local temperature factor which appears on the left-hand side of Eq. (14'). This assumption is plausible if we note that Σ represents the correlation of microscopic processes which are supposed to be local to the surface.

Performing the integration in Eq. (14) results in

$$\begin{aligned} \frac{\langle \tilde{\rho}(x, \vec{k}_{||}, \omega) \tilde{\rho}^*(x', \vec{k}_{||}, \omega) \rangle_{\text{NE}}}{2k_B \rho_0 \alpha} &= \frac{1}{|c_\omega^2|^2} T(x) \delta(x-x') + \frac{i\omega}{2\alpha |c_\omega^2|^2} \left[\frac{c_\omega^{*2}}{c_\omega^2} T(x') G(x|x') - \frac{c_\omega^2}{c_\omega^{*2}} T(x) G^*(x|x') \right] \\ &+ \frac{\nabla T}{2\alpha^2 \omega^2} \left[\frac{\partial}{\partial x'} G(x|x') + \frac{\partial}{\partial x} G^*(x|x') \right] + \frac{\nabla T}{2\alpha^2} \left[\frac{c_0^4}{|c_\omega^2|^2} + |\beta|^2 - \frac{c_0^2 k_{||}^2}{\omega^2} \right] \\ &\times [G(x|-L/2) G^*(x'|-L/2) - G(x|-L/2) G^*(x'|L/2)] + \frac{1}{|c_\omega^2|^2} \left[\frac{\Sigma}{\alpha} - \frac{\omega}{2\alpha c_0} \text{Re}\beta \right] \\ &\times [T(L/2) G(x|L/2) G^*(x'|L/2) + T(-L/2) G^*(x'|-L/2)]. \end{aligned} \quad (15)$$

The manipulations leading to Eq. (15) are straightforward, and the algebraic details are omitted. In equilibrium, the density correlation function becomes

$$\begin{aligned} \frac{\langle \tilde{\rho}(x, \vec{k}_{||}, \omega) \tilde{\rho}^*(x', \vec{k}_{||}, \omega) \rangle_{\text{eq}}}{2k_B \rho_0 \alpha} &= \frac{T_0}{|c_\omega^2|^2} \delta(x-x') + \frac{i\omega T_0}{2\alpha |c_\omega^2|^2} \left[\frac{c_\omega^{*2}}{c_\omega^2} G(x|x') - \frac{c_\omega^2}{c_\omega^{*2}} G^*(x|x') \right] \\ &+ \frac{T_0}{|c_\omega^2|^2} \left[\frac{\Sigma}{\alpha} - \frac{\omega^2}{2\alpha c_0} \text{Re}\beta \right] [G(x|L/2)G^*(x'|L/2) \\ &+ G(x|-L/2)G^*(x'|-L/2)]. \end{aligned} \quad (16)$$

The requirement that the equilibrium correlation function be even under time-reversal symmetry can only be satisfied if the coefficient of the last term in Eq. (16) vanishes, that is if $\Sigma = (\omega^2/2c_0) \text{Re}\beta$. The ω^2 dependence in Σ is not unreasonable, as the correlation function [cf. Eq. (14')] must be even in ω , and must vanish as $\omega \rightarrow 0$ [see Eq. (8)]. With this choice for Σ , the nonequilibrium density correlation function becomes

$$\begin{aligned} \frac{\langle \tilde{\rho}(x, \vec{k}_{||}, \omega) \tilde{\rho}^*(x', \vec{k}_{||}, \omega) \rangle_{\text{NE}}}{2k_B \rho_0 \alpha} &= \frac{1}{|c_\omega^2|^2} T(x) \delta(x-x') + \frac{i\omega}{2\alpha |c_\omega^2|^2} \left[\frac{c_\omega^{*2}}{c_\omega^2} T(x') G(x|x') - \frac{c_\omega^2}{c_\omega^{*2}} T(x) G^*(x|x') \right] \\ &+ \frac{\nabla T}{2\alpha^2 \omega^2} \left[\frac{\partial}{\partial x'} G(x|x') + \frac{\partial}{\partial x} G^*(x|x') \right] \frac{\nabla T}{2\alpha} \left[\frac{c_0^4}{|c_\omega^2|^2} + |\beta|^2 - \frac{c_0^2 k_{||}^2}{\omega^2} \right] \\ &\times [G(x|-L/2)G^*(x'|-L/2) - G(x|L/2)G^*(x'|L/2)]. \end{aligned} \quad (17)$$

As mentioned before, elastic theory predicts very small values for β . The effects of surface roughness can be modeled phenomenologically by using a larger β .¹⁴ In this case, phonons impinging on a rough surface scatter with a random distribution of scattering angles (i.e., Snell's Law for the effective flat surface is not obeyed). Looking only at the specular angle, there would appear to be a loss in coherent intensity. This effect is important only when the wavelength of the phonon is comparable to the scale of the surface roughness, i.e., for sufficiently large ω .

In the surface layer, Eq. (5) is too simple and boundary conditions must be imposed at the true surface. If one could carry out the mathematics, it would be more realistic to solve the full fluctuating hydrodynamic equations with boundary conditions specified on the rough surface. The solution would then be asymptotically matched to that given by Eq. (2). This would allow us to compute $\tilde{\sigma}$ and β . In this approach, the random sources in the surface layer would not correlate with τ in the bulk. Since Eq. (2) does not hold inside the surface layer, its source term τ should be irrelevant. Since the fluctuations in the surface layer will not be bulklike, we set τ (which is a bulklike source term) to zero in the

surface layer, the true physics being absorbed in $\tilde{\sigma}$. From the above discussion, it is reasonable to assume

$$\begin{aligned} \left\langle \tilde{\tau}(x, \vec{k}_{||}, \omega) \tilde{\sigma}^* \left[\frac{L}{2}, \vec{k}_{||}, \omega \right] \right\rangle_{\text{NE}} &= 0, \\ \left\langle \tilde{\sigma} \left[\frac{L}{2}, \vec{k}_{||}, \omega \right] \tilde{\sigma}^* \left[-\frac{L}{2}, \vec{k}_{||}, \omega \right] \right\rangle_{\text{NE}} &= 0, \\ \left\langle \tilde{\sigma} \left[\pm \frac{L}{2}, \vec{k}_{||}, \omega \right] \tilde{\sigma}^* \left[\pm \frac{L}{2}, \vec{k}_{||}, \omega \right] \right\rangle_{\text{NE}} \\ &= 2k_B \rho_0 \Sigma T(\pm L/2). \end{aligned}$$

These phenomenological correlations, when used in Eq. (14'), together with the fluctuation dissipation relation for Σ gives

$$\begin{aligned} \left\langle \tilde{\sigma} \left[\pm \frac{L}{2}, \vec{k}_{||}, \omega \right] \tilde{\sigma}^* \left[\pm \frac{L}{2}, \vec{k}_{||}, \omega \right] \right\rangle_{\text{NE}} \\ = \frac{k_B \rho_0 \omega^2 \text{Re}\beta}{c_0} T(\pm L/2). \end{aligned} \quad (18)$$

Note that this in no way changes the observable quantity, the density correlation function.

III. LIGHT-SCATTERING SPECTRUM

The intensity of scattered light is given by¹⁵

$$I = c \int_{\nu} d\vec{r}' \int_{\nu} d\vec{r} e(\vec{r}) e^*(\vec{r}') e^{-i\vec{k} \cdot (\vec{r} - \vec{r}')} \times \langle \rho(\vec{r}, \omega) \rho^*(\vec{r}', \omega) \rangle, \quad (19)$$

where $e(\vec{r})$ specifies the profile of the light source, and c is a constant. As the fluid is homogeneous in the y and z directions, we take $e(\vec{r}) = e(x)$. For a Gaussian profile, we have

$$e(\vec{r}) \propto \frac{1}{d} e^{-(x-x_0)^2/2d^2}. \quad (20)$$

If the beam is narrow on the scale of L , we may extend the limits of the x integrations in Eq. (19) to infinity with only exponentially small error. Note that this approximation will yield incorrect results if $|x_0| - L/2$ is less than the width of the beam. With these approximations, substitution of (17) and (20) into (19) yields, after straightforward but tedious integration,

$$\begin{aligned} I \propto & \frac{\alpha}{|c_{\omega}^2|^2} \sqrt{\pi} T(x_0) \\ & + \text{Re} \left\{ \frac{i\pi\omega d}{2|c_{\omega}^2|^2 \kappa \sin\kappa\lambda} \frac{c_{\omega}^{*2}}{c_{\omega}^2} \left\{ \left[e^{-d^2(q+\kappa)^2} \left[T(x_0) + d^2(q+\kappa)\nabla T + \frac{\kappa c_{\omega}^4}{\alpha\omega^3} \nabla T \right] f(q, \kappa) \right] \right. \right. \\ & \left. \left. + \left[e^{-d^2(q-\kappa)^2} \left[T(x_0) + d^2(q-\kappa)\nabla T - \frac{\kappa c_{\omega}^4}{\alpha\omega^3} \nabla T \right] f(-q, \kappa) \right] \right. \right. \\ & \left. \left. + e^{-d^2(q^2+\kappa^2)} \left[[T(x_0) - iq d^2 \nabla T] \cos 2\kappa x_0 + \left[d^2\kappa + \frac{i\kappa c_{\omega}^4}{\alpha\omega^3} \right] \nabla T \sin 2\kappa x_0 \right] \right\} \right\} \\ & + \pi d \nabla T \frac{(\kappa^2 + \kappa^*)^2 |\cos\kappa\phi|^2 + 2|\kappa|^2 |\sin\kappa\phi|^2}{2\alpha\omega^2 |\kappa \sin\kappa\lambda|^2} \\ & \times \text{Im} \left[\sin(\kappa\lambda/2) \cos(\kappa^* \lambda^*/2) (e^{i\kappa x_0 - d^2(q+\kappa)^2/2} - e^{-i\kappa x_0 - d^2(q-\kappa)^2/2}) \right. \\ & \left. \times (e^{i\kappa^* x_0 - d^2(q-\kappa^*)^2/2} + e^{-i\kappa^* x_0 - d^2(q+\kappa^*)^2/2}) \right], \quad (21) \end{aligned}$$

where q is the \hat{x} component of \vec{k} and

$$\frac{\lambda}{2} = L/2 - \phi$$

$$f(q, \kappa) = \frac{1}{2} \{ \cos\kappa\lambda - i \sin\kappa\lambda \text{erf}[id(q+\kappa)] \}.$$

From Eq. (21) two features of the spectrum are easily seen. First, the line shapes are essentially Gaussian with width determined by the parameters

of the light source. Second, the intensity of scattered light will be particularly large when $\text{Re}(\sin\kappa L)$ vanishes. These resonances, which occur whenever $\omega = n\pi c/L$, are a result of scattering from the (fluctuating) standing-wave pattern (i.e., cavity modes) established between the boundary plates. In addition, it can easily be shown that Eq. (21) reduces to the usual result¹⁻⁹ when $L \rightarrow \infty$ or $q \rightarrow \infty$. [Specifically, the resonances disappear. The overall line shape is still Gaussian until $l(q) \ll d$, in which case a square-Lorentzian line-shape results.]

IV. RESULTS AND DISCUSSION

In this section, the analytic expression for the light-scattering intensity [Eq. (21)] is evaluated, and the asymmetry ratio ϵ is obtained by numerically integrating the spectrum. For concreteness, we have chosen our parameters to correspond to those of Beysens's experiments (i.e., water at 313 K, with $\nabla T = 59$ K/cm). For this system, the sound velocity $c_0 = 153\,000$ cm/sec, the sound attenuation coefficient $\alpha = 2.6 \times 10^{-2}$ cm²/sec, the distance between plates $L = 0.515$ cm, and the beam halfwidth $d = 0.01$ cm. Note that the small size of the system

improves the approximation that the parameters are temperature independent.

Figures 1(a)–1(c) present theoretical spectra for a typical value of q for a variety of acoustic impedences. There are three main features: (1) the Gaussian line shape of each of the Brillouin peaks, reflecting our choice of a Gaussian beam; (2) the standing wave resonances, occurring whenever $\omega L/c_0 = n\pi$; (3) the increase in asymmetry with increasing β . It is interesting to note that the total intensity is independent of β . If no surface sources were included, we would expect a decrease with increasing β . The surface sources precisely compen-

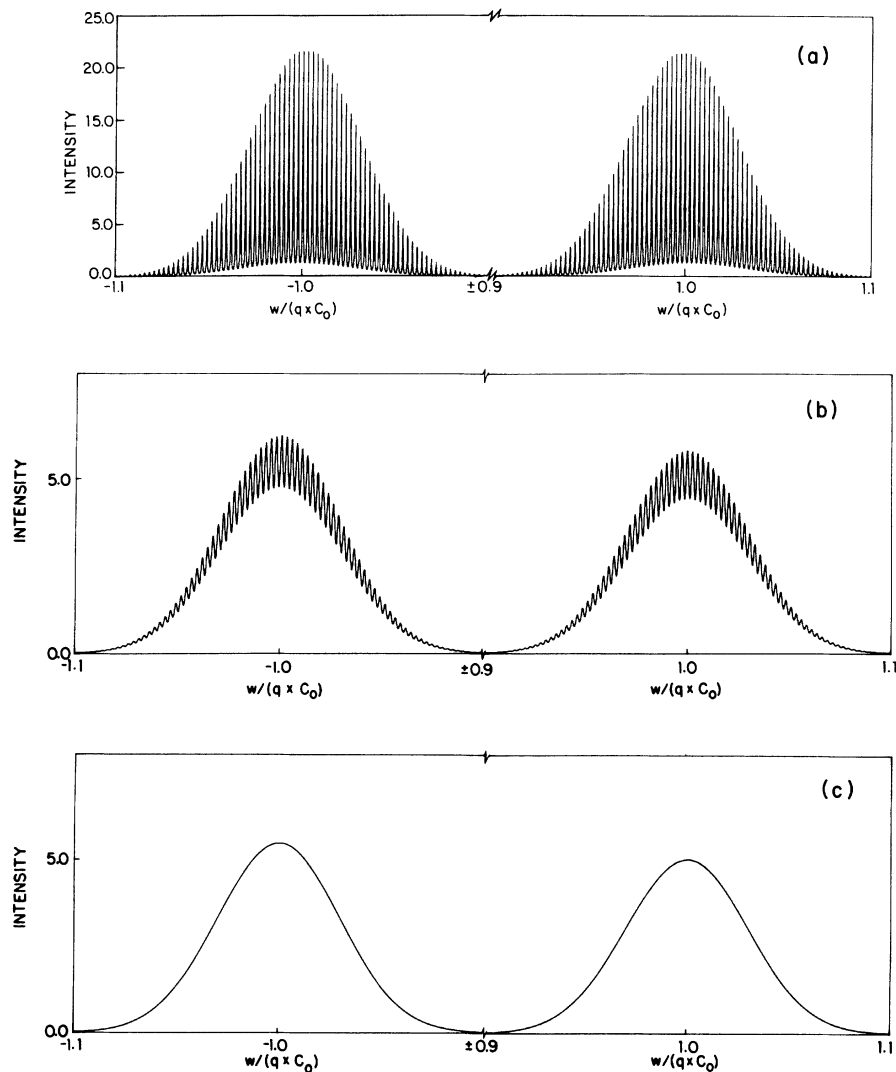


FIG. 1. Typical spectra for $q = 2380$ cm⁻¹, $L = 0.515$ cm, and $\nabla T = 59$ K/cm in water at 313 K. (a)–(c) show the effect of changing β (0.0, 0.5, and 1.0, respectively). Envelope of the peaks is a Gaussian whose width is determined by the beam diameter ($d = 0.01$ cm and $x_0 = 0.0$). Total integrated intensities are independent of β .

sate for this tendency.

That the line shape is determined by the beam profile is not surprising. Light-scattering probes spatial coherence, and in the cases considered in this paper, the (hydrodynamic) correlation length ($l=2c_0/\alpha k^2$) is much larger than the beam diameter, making it irrelevant to the overall line shape.

The standing-wave patterns would be extremely difficult to resolve experimentally, as $\Delta\omega \sim 10^5$ Hz. Note that the width of the resonances increases with α and β . The dependence on β is quite strong, and as the limit of perfectly absorbing walls is reached ($\beta \rightarrow 1$) the resonances disappear. In addition, we have assumed that the frequency and parallel components of the wave vector are exactly resolved. In an actual experiment, this is only approximately true and hence the standing-wave resonance pattern (as determined by the minima of $|\sin(\kappa\lambda)|^2$) must be convolved with the appropriate incident parallel wave number ($k_{||}$) and frequency (ω) profiles. These factors will complicate the resolution of the standing-wave resonances.

In Fig. 2, the increase of ϵ with β exhibited qualitatively in Figs. 1(a)–1(c) is presented quantitatively for a variety of sample sizes. For perfectly reflecting walls, only the attenuation of sound prevents the total vanishing of ϵ . For a small system, the sound attenuation before reflection is minimal, and a large reduction in ϵ is found. (For water under the above conditions, the system must be ~ 10 cm for the bulk limit to be achieved.) As the walls become more absorbing the asymmetry increases, as there are fewer reflected phonons. Note, however, that even in the limit of perfectly absorbing walls, ϵ does not attain its bulk value. In a bulk

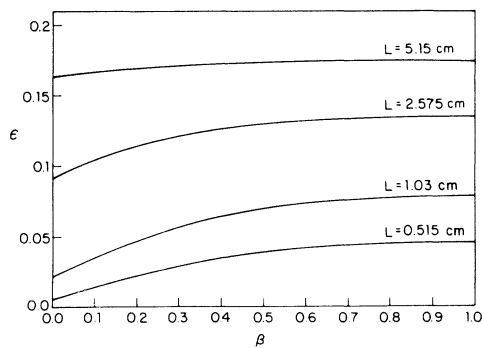


FIG. 2. Dependence of the intensity asymmetry ϵ on the surface admittance β for a variety of sample sizes. Other parameters are as in Fig. 1. Infinite-system limit is $\epsilon=0.196$. Acoustic reflection coefficient is given by $R=(1-\beta)/(1+\beta)$.

system, scattering occurs from phonons originating in the region $x_0 \pm l$ characterized by $T(x_0-l) \leq T \leq T(x_0+l)$. In a sufficiently small system, the restriction that fluctuations must originate in a region characterized by $T(-L/2) \leq T \leq T(L/2)$ reduces the number of phonons available for scattering, in particular, eliminating those phonons generated in the region having the highest (in the hot direction) and lowest (in the cold direction) source intensity. Note that for the conditions of Beysens's *et al.* experiments this effect is large (see Fig. 2).

In Fig. 3, we examine the dependence of ϵ on x_0 (beam center) for totally reflecting and totally absorbing walls. When the surface source terms are included, only a very weak x_0 dependence is found (solid line). Neglecting these terms leads to a spurious x_0 dependence (dashed line) which persists even in equilibrium. This dependence can be explained by noting that for highly reflecting walls, the $\omega = -qc_0$ peak is generated primarily by fluctuations originating at $x > x_0$, while the $\omega = +qc_0$ peak is generated primarily by fluctuations originating at $x < x_0$. Without surface sources, ϵ is determined largely by the volume of fluid above and below x_0 , even in equilibrium. The boundary sources compensate for this.

In Fig. 4, the dependence of ϵ on q is examined. For q less than some crossover value q_c , ϵ varies weakly with q . If q is greater than q_c , ϵ is correctly predicted by Eq. (1). The crossover value q_c can be determined by noting that the ratio L/l depends on q . We have seen previously (see, e.g., Fig. 2) that ϵ does not exhibit its bulk limit behavior unless $L \gtrsim 2l$. Using this, we find that $q_c \sim \sqrt{4c_0/\alpha L}$,

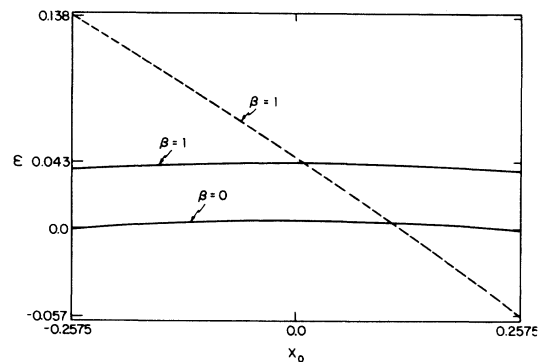


FIG. 3. Dependence of ϵ on x_0 , the position of the beam center, with (solid line) and without (dashed line) surface source terms. Recall that for $\beta=0$ surface source terms are irrelevant. All other parameters are as in Fig. 1.

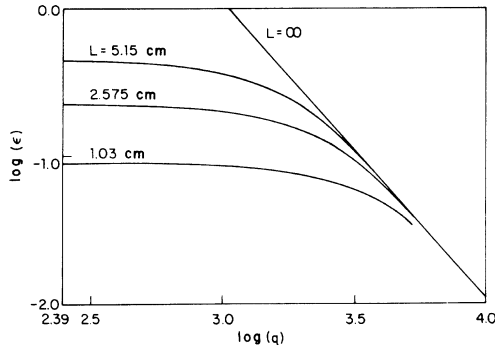


FIG. 4. Dependence of ϵ on the scattering wave vector q for $\beta=0.5$ ($R=\frac{1}{3}$) for a variety of system sizes. Note the strong deviation from $1/q^2$ behavior at small q .

which gives reasonable agreement with Fig. 3. Note that the behavior of ϵ below q_c indicates that the surfaces quench the long-range correlation of the infinite system as soon as the fluctuations interact with the surface. From an experimental point of view, note that the behavior below q_c obviates the need for ever smaller angle scattering to enhance the asymmetry of the Brillouin peaks.

Linear theories with constant-temperature gradients based on infinite fluids break down in the limit $k \rightarrow 0$ ($l \rightarrow \infty$), because some phonons contributing to the light scattering will have been generated in regions of negative temperature, thus leading to negative spectra.^{6(c)} Note, however, that this is not the case for our theory, and that as long as the temperature in the cell is positive, the spectra will always be positive.

Table I contains a comparison of experimental results with results calculated by the theory in this paper and by Eq. (1). For relatively large β , the

agreement between our results and experiment is well within the scatter in the experimental results. As the scale of the surface roughness was not small compared to the phonon wavelength in the experiments, a large β is expected.

For the temperature gradient used here, it is of course ridiculous to consider too large a cell. Nonetheless, this is a linear theory and all asymmetries can be easily rescaled for a smaller temperature gradient.

V. CONCLUDING REMARKS

Kirkpatrick and Cohen⁹ have proposed a nonlinear mechanism in an infinite system whereby ϵ can be decreased. As we have shown, a linear theory with boundary effects also results in a decrease in ϵ . Since boundaries tend to weaken the effects of nonlinearities (i.e., there is not enough room for them to develop) we expect that for a sufficiently small system the effect of the boundaries will be dominant. The parameter characterizing nonlinearities in Kirkpatrick and Cohen's theory is $l(\nabla T/T)$, while the effect of the boundaries is measured by l/L . Thus, for sound, the ratio of the influence of nonlinearities to boundary effects is given by $L\nabla T/T \equiv \Delta T/T$, where ΔT is the temperature difference between top and bottom surfaces. Except at extremely low temperature, this ratio is small. In particular, for Beysens *et al.* experiment, this ratio $\Delta T/T \approx 0.1$; hence, the effect of boundaries should be much greater than any nonlinear effects. This does not necessarily imply that nonlinearities can always be neglected, but rather that nonlinearities must be considered along with boundary conditions. We expect that the nonlinear mechanism will become more important as the size of the system is in-

TABLE I. Comparison of theoretical and experimental asymmetries.

q	∇T	$\epsilon(\beta=0) \times 10^2$	$\epsilon(\beta=0.5) \times 10^2$	$\epsilon(\beta=1) \times 10^2$	$\epsilon(\text{expt}) \times 10^2$	$\epsilon \times 10^2$ [linear theory, Eq. (1)]
3420	59	1.08	3.38	3.77	7.5	9.4
3360	59	1.05	3.40	3.80	4.3	9.8
3220	59	0.98	3.44	3.87	3.5	10.6
3130	59	0.93	3.47	3.92	3	11.2
2380	59	0.56	3.65	4.27	11.74	19.4
2110	59	0.44	3.70	4.38	8.84	24.7
3060	83	1.26	4.91	5.57	6.25	16.7
2100	84	0.62	5.27	6.25	7.92	35.8
2720	92	1.13	5.58	6.43	7.38	23.4
2590	93	1.04	5.69	6.59	3.93	26.1

creased.

To summarize, we have shown that finite-size effects can cause a substantial reduction in the asymmetry of the Brillouin peaks from that previously calculated for infinite systems. This reduction is present even for totally absorbing walls, and leads to reasonable agreement between linear theory and Beysens *et al.* experimental data. In addition, we have shown that the line shape of the Brillouin peaks is determined by the characteristics of the light source, with an added resonant substructure dependent on the boundaries.

ACKNOWLEDGMENTS

A portion of this work was supported by a Cottrell Research Grant from the Research Corporation. One of us (G. S.) acknowledges the support of the National Science Foundation Graduate Fellowship Program. We would also like to thank Isaac Goldhirsch for useful discussions. We appreciate Claude and Andre-Marie Tremblay's pointing out the scaling argument used in the concluding remarks.

¹D. Ronis, I. Procaccia, and J. Machta, *Phys. Rev. A* **22**, 714 (1980).

²(a) A.-M. S. Tremblay, M. Arai, and E. D. Siggia, *Phys. Lett.* **76A**, 57 (1980); (b) *Phys. Rev. A* **23**, 1451 (1981).

³D. Ronis and S. Putterman, *Phys. Rev. A* **22**, 773 (1980).

⁴(a) G. Van der Zwan and P. Mazur, *Phys. Lett.* **75A**, 370 (1980); (b) G. Van der Zwan, D. Bedeaux, and P. Mazur, *Physica (Utrecht)* **107A**, 491 (1981).

⁵A.-M. S. Tremblay and C. Tremblay, *Phys. Rev. A* **25**, 1692 (1982).

⁶(a) I. Procaccia, D. Ronis, and I. Oppenheim, *Phys. Rev. Lett.* **42**, 287 (1979); (b) I. Procaccia, D. Ronis, M. A. Collins, J. Ross, and I. Oppenheim, *Phys. Rev. A* **19**, 1290 (1979); (c) D. Ronis, I. Procaccia, and I. Oppenheim, *ibid.* **19**, 1307 (1979); **20**, 2533 (1979).

⁷I. Oppenheim, in *Molecular Structure and Dynamics*, edited by M. Balabau (International Science Services, Jerusalem, Israel, 1980), p. 3.

⁸(a) T. Kirkpatrick, E. G. D. Cohen, and J. R. Dorfman, *Phys. Rev. Lett.* **42**, 862 (1979); **44**, 472 (1980); (b) T.

Kirkpatrick, Ph.D. thesis, The Rockefeller University, 1981 (unpublished).

⁹T. Kirkpatrick and E. G. D. Cohen, *Phys. Lett.* **78A**, 350 (1980).

¹⁰(a) D. Beysens, Y. Garrabos, and G. Zalczer, *Phys. Rev. Lett.* **45**, 403 (1980); (b) D. Beysens (unpublished).

¹¹L. D. Landau and E. M. Lifshitz, *Fluid Mechanics* (Pergamon, New York, 1959), Chap. XVII.

¹²The need for surface fluctuating sources when dissipative boundary conditions are used has been discussed, for Brownian motion, by D. Bedeaux, A. M. Albano, and P. Mazur, *Physica (Utrecht)* **88A**, 574 (1977).

¹³K. M. van Vliet, A. van der Ziel, and R. R. Schmidt, *J. Appl. Phys.* **51**, 2947 (1980).

¹⁴See, e.g., A. D. Pierce, *Acoustics: An Introduction to its Physical Principles and Applications* (McGraw-Hill, New York, 1981).

¹⁵R. Edwards, J. Angus, M. French, and J. Dunning, *J. Appl. Phys.* **42**, 837 (1971).